Herschel/SPIRE observations of water production rates and ortho-to-para ratios in comets[*]

Thomas G. Wilson,[1]† Jonathan M. C. Rawlings[1] and Bruce M. Swinyard[1,2]‡

[1]*Department of Physics & Astronomy, University College London, Gower Street, London WC1E 6BT, UK*
[2]*RAL Space, Science & Technology Facilities Council, Rutherford Appleton Laboratory, Chilton, Didcot, Oxon OX11 0QX, UK*

ABSTRACT

This paper presents *Herschel*/SPIRE (Spectral and Photometric Imaging Receiver) spectroscopic observations of several fundamental rotational ortho- and para-water transitions seen in three Jupiter-family comets and one Oort-cloud comet. Radiative transfer models that include excitation by collisions with neutrals and electrons, and by solar infrared radiation, were used to produce synthetic emission line profiles originating in the cometary coma. Ortho-to-para ratios (OPRs) were determined and used to derived water production rates for all comets. Comparisons are made with the water production rates derived using an OPR of 3. The OPR of three of the comets in this study is much lower than the statistical equilibrium value of 3; however they agree with observations of comets 1P/Halley and C/2001 A2 (LINEAR), and the protoplanetary disc TW Hydrae. These results provide evidence suggesting that OPR variation is caused by post-sublimation gas-phase nuclear-spin conversion processes. The water production rates of all comets agree with previous work and, in general, decrease with increasing nucleocentric offset. This could be due to a temperature profile, additional water source or OPR variation in the comae, or model inaccuracies.

Key words: molecular processes – radiative transfer – techniques: spectroscopic – comets: general – comets: individual: 103P/Hartley 2, 10P/Tempel 2, 45P/Honda–Mrkos–Pajdušáková, C/2009 P1 (Garradd) – submillimetre: general.

1 INTRODUCTION

As comets are formed and spend most of their lifetimes in the outer Solar system they do not undergo significant thermal processing and therefore retain pristine material from the solar protoplanetary disc. Thus studying comets can reveal the history and evolution of the Solar system. Water is the most abundant volatile in cometary nuclei and its sublimation produces much of the activity seen as comets entering the inner Solar system (heliocentric distance, r_h, ≤ 3 au). By studying water in comets, comparisons can be made with exoplanetary systems and protoplanetary discs, and a better understanding of planetary formation can be achieved. The ortho-to-para ratio (OPR) of water has been of great interest in recent years in studies looking to understand the history and thermal processing of water in various regions, such as the interstellar medium, star-forming regions and a protoplanetary disc (Lis et al. 2013a; Choi et al. 2014; Salinas

et al. 2016). Notably, there is continuing debate as to what fraction of the terrestrial water reservoir was delivered to the Earth by cometary impacts, with key evidence being provided by isotopic ratios such as D/H in cometary ices (Altwegg et al. 2015; Bockelée-Morvan et al. 2015; Willacy et al. 2015). By determining water production rates, Q_{H_2O}, the physical conditions in cometary comae such as temperature, expansion velocity and excitation conditions can be understood. From constraining the relative abundances of other volatiles compared to water, conditions in the protoplanetary disc and early outer Solar system can be determined. Moreover, the comet-to-comet Q_{H_2O} variation (and particularly if there is any distinction between Jupiter-family and Oort-cloud comets) can potentially provide information about the evolution and origin of the cometary ices. Water molecules in cometary comae are excited collisionally by neutrals and electrons, and by solar infrared radiative pumping of fundamental vibration levels. These excitation methods predominantly occur between fundamental rotational levels as cometary comae are typically rotationally cold environments. The majority of the strongest rotational lines, and those mentioned below, are observed in the submillimetre and therefore space-based missions like the *Herschel Space Observatory* provide excellent opportunities for studying the physical properties of comae.

The first direct detection of water in comets was observed in comet 1P/Halley by the Kuiper Airborne Observatory. Fundamental rotational transitions, $2_{12} - 1_{01}$ and $3_{03} - 2_{12}$, were first observed by the *Infrared Space Observatory* (*ISO*) in comet C/1995 O1 (Hale–Bopp) (Crovisier et al. 1997). Subsequent space-based missions have detected the fundamental $2_{12} - 1_{01}$ ortho-water line with the *Submillimeter Wave Astronomical Satellite* (Neufeld et al. 2000), *Odin* (Lecacheux et al. 2003; Biver et al. 2007, 2009) and *Herschel* (Hartogh et al. 2010; Biver et al. 2012). Observations with *Herschel* have also detected the $2_{12} - 1_{01}$ ortho, and $1_{11} - 0_{00}$ and $2_{02} - 1_{11}$ para-water transitions (de Val-Borro et al. 2010, 2012, 2014; Szutowicz et al. 2011; Bockelée-Morvan et al. 2012; Lis et al. 2013b). Multiple water rotational lines have been observed by *Rosetta* after the initial detection of the $2_{12} - 1_{01}$ transition (Gulkis 2014).

For molecules with two protons, each with a nuclear-spin angular momentum $I = 1/2$, two nuclear-spin isomers exist: ortho ($I = 1$, triplet) and para ($I = 0$, singlet). Due to the Pauli principle ortho-water exists in rotational states with odd $K_a + K_c$ and para-water with even $K_a + K_c$, as can be seen in Fig. 2, where $K_a + K_c$ are the projections of the total angular momentum quantum number, J, on to the principal a and c axes. As can be seen in Fig. 2 the lowest ortho- and para-water levels have a rotational energy difference of 34.2 K that leads to para-water being more stable in the gas-phase and therefore the OPR can be used as a probe of low-temperature regions.

For observations of multiple water rotational lines of both ortho- and para-water transitions the OPR can be determined from equation (1), where the OPR is determined as the ratio of sum of all the ortho line intensities divided by their branching ratios, with the sum of all the para line intensities divided by their branching ratios.

$$\mathrm{OPR} = \frac{\sum_i I_o(i)/B_o(i)}{\sum_j I_p(j)/B_p(j)} \tag{1}$$

where i, j indicate individual lines, ortho- and para-intensities are $I_o(i)$ and $I_p(j)$, respectively, and $B_o(i)$ and $B_p(j)$ are the ortho- and para-branching ratios for each transition.

Typically, the OPR in comets is 2.5–3.0; however multiple comets have been observed with OPR values lower than this and, interestingly, recent studies have reported OPR values in the interstellar medium, star-forming regions and a protoplanetary disc significantly lower than 3 (Lis et al. 2013a; Choi et al. 2014; Salinas et al. 2016). From the OPR the nuclear-spin temperature can be determined (Mumma, Weaver & Larson 1987).

Nuclear-spin conversion between isomers of isolated molecules occurs very rarely due to the weak magnetic interactions between intramolecular nuclear spins. However, through hydrogen- or proton-exchange reactions via intermolecular interactions or the mixing of nuclear-spin states via perturbations nuclear-spin conversion can occur. Nuclear-spin conversion can occur collisionally in the gas-phase via the quantum-relaxation model (Hama & Watanabe 2013). If, following a collision, an ortho-water molecule is closer to a para state then coherent mixing of ortho and para states via internal perturbations occurs. A following collision accounts for energy relaxation and the ortho to para conversion is complete.

It has been proposed that in the solid-phase nuclear-spin conversion also occurs through intermolecular spin-magnetic-dipole interactions with neighbouring water molecules on the time-scale of 10^{-5}–10^{-4} s. This rapid conversion is due to the rotational energy difference between ortho and para levels decreasing substantially to 5×10^{-13} K in the solid-phase as there is high barrier for rotation due to hydrogen bonds (Buntkowsky et al. 2008).

The interpretation of the OPR has been long debated and historically the nuclear-spin temperature was thought to be indicative of the comet ice formation temperature and therefore comet formation location (Mumma et al. 1987). However, a recent laboratory study has observed that the OPR of both vapour-deposited and in situ-produced water that is sublimated either by thermal desorption at 150 K or by photodissociation at 10 K is equal to a value of 3 (Hama, Kouchi & Watanabe 2016). This study shows that rapid solid-phase nuclear-spin conversion occurs in water ice and normalizes the OPR to the statistical equilibrium. Furthermore, the sublimation processes used in the experiment did not alter the OPR. Therefore, the OPRs observed in cometary comae are not indicative of the formation temperature of the cometary ices, but instead probe the gas-phase physical conditions in comae.

Although it has been predicted that the collision rate of water with other water molecules, ions and electrons is too small to induce efficient nuclear-spin conversion in cometary comae (Crovisier 1984; Mumma et al. 1987), it has been suggested that comae OPR variation could be due to proton-transfer reactions of water with H^+ and H_3O^+, via water molecule collision with water clusters, or by interactions with ice grains and paramagnetic dust grains in the collisional, fluid, coma regions near the nucleus via the quantum relaxation model described previously (Irvine et al. 2000; Hama & Watanabe 2013; Manca Tanner, Quack & Schmidiger 2013). Therefore, nuclear-spin conversion, especially in the low-temperature conditions of the coma, needs to be re-examined in order to interpret the observed OPRs.

A recent study of ammonia in 26 comets found a correlation between the ammonia and water nuclear-spin temperatures potentially suggesting a common process of OPR, and therefore nuclear-spin temperature, variation.

Observations of 103P/Hartley 2, 10P/Tempel 2, 45P/Honda–Mrkos–Pajdušáková and C/2009 P1 (Garradd) were undertaken between 2010 July 10 and 2011 October 16 with the Spectral and Photometric Imaging Receiver (SPIRE) (Griffin et al. 2010) instrument onboard *Herschel* (Pilbratt et al. 2010), in the framework of the *Herschel* Guaranteed Time Key project 'Water and related chemistry in the Solar system' (HssO) (Hartogh et al. 2009). The observations are presented in Section 2 and data analysis including the modelling and results are reported in Section 3. The main points of the study are discussed in Section 4 and conclusions are given in Section 5.

2 OBSERVATIONS

The spectra of the comets were acquired with the SPIRE Fourier Transform Spectrometer (FTS) (Swinyard et al. 2014) that covers the spectral range 447–1568 GHz with the short (SSW, 191–318 μm) and long (SLW, 294–671 μm) wavelength channels. The observations were taken in high-resolution mode with a spectral resolution of $\Delta \nu = 1.2$ GHz ($\lambda/\Delta\lambda = 1000$ at $\lambda = 250$ μm). In order to study the comae of the comets the SSW and SLW central bolometers were ignored, effectively creating two rings of SSW beams offset from the nucleus by roughly 33 and 66 arcsec and a ring of SLW beams offset from the nucleus by approximately 51 arcsec (Herschel Science Centre. 2014). The physical offset distance in km is given in Table 2. The purpose of studying these SPIRE observations was to determine the OPR and Q_{H_2O} values in the

Table 1. Orbital and physical properties, and model parameters.

	r_n (km)	P (yr)	v_{exp} (km s^{-1})	β_{H_2O} (s^{-1})
Hartley 2	0.7	6.46	0.83	1.08×10^{-5}
Tempel 2	5.3	5.36	0.50	1.06×10^{-5}
45P	0.8	5.26	0.75	1.16×10^{-5}
C/2009 P1	<5.6	127,000	0.60	1.16×10^{-5}

comae of comets with different formation and evolution conditions at a range of nucleocentric distances.

Data processing was done in HIPE 13.0 using the standard SPIRE scripts. Background subtraction, estimated from the off-axis detectors, and frequency-based mask fitting scripts were also used on Tempel 2, 45P and C/2009 P1, to produce a better behaved and flatter continuum from which the line intensities were read.

The JPL HORIZONS system was used to calculate the comet positions and relative motions with respect to *Herschel* and the spectra were corrected for the respective *Herschel*-centric velocities. All observations were taken at offset distances greater than the recombination surface (Bensch & Bergin 2004).

The nucleus radius, r_n, and period, P, of each comet are given in Table 1. The $r_{h_{obs}}$, the *Herschel*-comet distance, Δ_{obs} and the time between observation and perihelion, ΔT_{obs}, where negative values are pre-perihelion and positive values are post-perihelion, when the observations were taken, are reported in Table 2.

2.1 103P/Hartley 2

103P/Hartley 2 (hereafter Hartley 2) is a Jupiter-family comet that passed perihelion on 2010 October 28 at $r_h = 1.059$ au, a week after making a close approach to the Earth on October 21 at $\Delta = 0.12$ au. Hartley 2 was the target of the EPOXI space mission on 2010 November 4 and was observed by 51 telescopes in a worldwide campaign (Meech et al. 2011). One SPIRE FTS observation was taken with a duration of 7002 s on 2010 November 9. As can be seen in Fig. 1 several fundamental rotational water emission lines were detected.

2.2 10P/Tempel 2

The Jupiter-family comet 10P/Tempel 2 (hereafter Tempel 2) passed perihelion on 2010 July 4 at $r_h = 1.42$ au shortly before the one SPIRE FTS observation that was taken on 2010 July 10 with a duration of 5650 s. Several fundamental rotational water emission lines were detected in Tempel 2 as can be seen in Fig. 1.

2.3 45P/Honda–Mrkos–Pajdušáková

Comet 45P/Honda–Mrkos–Pajdušáková (hereafter 45P) is a Jupiter-family comet that, on 2011 August 15, passed Earth with $\Delta = 0.06$ au before perihelion on 2011 September 28 ($r_h = 0.53$ au). After the next perihelion passage (2016 December 31) the comet will pass Earth at $\Delta = 0.08$ au on 2017 February 11, providing an opportunity for further observations. Fig. 1 shows the spectra obtained by the SPIRE FTS observation of 4568 s on 2011 August 16 with the observed fundamental rotational water lines noted.

2.4 C/2009 P1 (Garradd)

Comet C/2009 P1 (Garradd) (hereafter C/2009 P1) is a long period comet originating from the Oort cloud ($i = 106°$ with respect to

the ecliptic). The comet passed perihelion on 2011 December 23 at $r_h = 1.55$ au and was observed with the SPIRE FTS on 2011 October 16 for 4568 s. Fundamental rotational water emission lines can be seen in Fig. 1.

3 DATA ANALYSIS

3.1 Radiative transfer model

Analysis was carried out using the one-dimensional Accelerated Monte Carlo radiative transfer code; CRETE (de Val-Borro & Wilson 2016) that was inspired by RAT4COM (Bensch & Bergin 2004), and adapted from the previous work done to generate synthetic water emission spectra (Hogerheijde & van der Tak 2000). The model includes the excitation of water molecules via collisions with other water molecules and electrons in the inner coma, and by solar infrared pumping of the vibrational bands and fluorescence in the outer coma.

Previous studies concentrated on ortho-water, considering nine rotational transitions between the seven lowest levels in the ground vibrational state. The updated model also includes the radiative transfer for transitions between the seven lowest levels of para-water. The ortho- and para-water transitions in the updated model can be seen as blue arrows in Fig. 2, with green arrows representing transitions both in the model and observed in all the SPIRE detectors.

The spherically symmetric Haser distribution (Haser 1957) was used for the radial gas expansion profile and the expansion velocities were assumed to be constant in the cometary comae. This distribution is essentially applicable to a spherically symmetric, constant expansion velocity (v_{exp}), outflow (scaling as $1/r^2$), with an exponential decay term ($\exp(-r\beta_{H_2O}/v_{exp})$) that accounts for photodissociation (rate β_{H_2O}) and ionization by the solar radiation field.

The model parameters that are essentially constrained include r_h, Δ, and scaling factors for β_{H_2O} and the ionization rate that take into account the r_h and level of solar activity. Parameters that are reasonably well constrained and for which values from the literature were used include v_{exp}, the gas kinetic temperature (T_{kin}) and β_{H_2O}. The only free parameters are Q_{H_2O}, the electron density scaling factor (x_{n_e}), the contact surface scaling factor (x_{r_e}) and the number of shells in the radiative transfer calculations.

At the nucleocentric distances observed a constant $T_{kin} = 40$ K is assumed as previous work has shown this value to be a good approximation (Combi et al. 1999). Observations of the $1_{10} - 1_{01}$ (557 GHz) water line in other comets have constrained x_{n_e} to 0.2 (Biver 1997; Biver et al. 2007; Hartogh et al. 2010). Previous observations of 1P/Halley have shown that x_{r_e}, a scaling factor that determines the boundary radius between collisional excitation predominantly caused by water–water and water–electron, is equal to unity (Balsiger 1990; Festou 1990). The number of shells was set at 1500 based on recommendations (Bensch & Bergin 2004). Adopted values for the other model parameters mentioned above are given in Table 1.

Although this model makes some simplistic assumptions such as spherical symmetry of the outgassing, and in the irradiation and photochemistry of the water, the omission of vibrationally excited levels, and radiative transfer at infrared wavelengths a number of comet observations have been modelled with considerable success (Zakharov et al. 2007; Hartogh et al. 2010; Bockelée-Morvan et al. 2012).

Table 2. Coma averaged OPR values for the four *Herschel*/SPIRE comets. Q_{H_2O} determined for various lines and nucleocentric offsets using (i) the calculated OPR values and (ii) an OPR of 3.

Comet	Start date (UT) yyyy/mm/dd.dd	ΔT_{obs} (d)	$r_{h_{obs}}$ (au)	Δ_{obs} (au)	OPR	Transition	ν_{ij} (GHz)	Ortho /para	Offset (km)	Q_{H_2O} (10^{27} s^{-1}) (i)	(ii)
Hartley 2	2010/11/09.03	11.77	1.071	0.176	2.44 ± 0.71	$1_{10} - 1_{01}$	557	Ortho	6400	3.83 ± 0.12	3.61 ± 0.17
						$2_{11} - 2_{02}$	752	Para	6400	1.89 ± 0.11	2.19 ± 0.15
						$2_{02} - 1_{11}$	988	Para	4100	6.43 ± 0.13	7.49 ± 0.21
									6400	5.68 ± 0.11	6.57 ± 0.12
									8200	4.09 ± 0.15	4.75 ± 0.20
						$3_{12} - 3_{03}$	1097	Ortho	4100	0.55 ± 0.06	0.55 ± 0.06
									8200	0.35 ± 0.04	0.35 ± 0.04
						$1_{11} - 0_{00}$	1113	Para	4100	7.46 ± 0.13	8.67 ± 0.19
									8200	5.57 ± 0.14	6.44 ± 0.20
Tempel 2	2010/07/10.93	6.03	1.424	0.732	1.59 ± 0.23	$1_{10} - 1_{01}$	557	Ortho	27000	11.6 ± 1.7	9.5 ± 1.4
						$2_{11} - 2_{02}$	752	Para	27000	3.8 ± 1.2	5.7 ± 1.8
						$2_{02} - 1_{11}$	988	Para	17000	9.5 ± 1.2	14.5 ± 1.8
									27000	5.2 ± 0.6	8.2 ± 0.9
									35000	10.2 ± 1.7	15.8 ± 2.5
						$3_{12} - 3_{03}$	1097	Ortho	17000	2.9 ± 1.3	2.3 ± 1.1
									35000	2.2 ± 1.0	1.8 ± 0.8
						$1_{11} - 0_{00}$	1113	Para	17000	8.6 ± 0.9	13.1 ± 1.3
									35000	6.0 ± 1.0	9.2 ± 1.5
45P	2011/08/16.13	-44.65	1.002	0.061	2.00 ± 0.30	$1_{10} - 1_{01}$	557	Ortho	2400	1.22 ± 0.11	1.08 ± 0.09
						$2_{11} - 2_{02}$	752	Para	2400	0.37 ± 0.09	0.49 ± 0.12
						$2_{02} - 1_{11}$	988	Para	1500	1.25 ± 0.10	1.67 ± 0.14
									2400	0.94 ± 0.05	1.26 ± 0.06
									3100	0.68 ± 0.11	0.90 ± 0.15
						$3_{12} - 3_{03}$	1097	Ortho	1500	0.19 ± 0.05	0.16 ± 0.04
									3100	0.14 ± 0.05	0.13 ± 0.05
						$1_{11} - 0_{00}$	1113	Para	1500	1.53 ± 0.07	2.04 ± 0.10
									3100	0.67 ± 0.08	0.90 ± 0.11
C/2009 P1	2011/10/16.79	-68.89	1.807	1.875	1.36 ± 0.22	$1_{10} - 1_{01}$	557	Ortho	69000	255 ± 10	196 ± 8
						$2_{11} - 2_{02}$	752	Para	69000	22 ± 6	37 ± 11
						$2_{02} - 1_{11}$	988	Para	45000	110 ± 6	187 ± 10
									69000	97 ± 3	164 ± 6
									90000	87 ± 14	147 ± 16
						$3_{12} - 3_{03}$	1097	Ortho	45000	17 ± 4	13 ± 3
									90000	21 ± 7	16 ± 6
						$1_{11} - 0_{00}$	1113	Para	45000	115 ± 5	195 ± 8
									90000	69 ± 12	116 ± 15

3.2 Ortho-to-para ratios

As mentioned in Section 1 due to the multiple transitions seen in the observations OPR values can be calculated using equation (1) and knowledge of the OPR of a comet can lead to the determination of the nuclear-spin temperature. Note that many of the upper levels of these transitions are populated from higher levels that are not included in the radiative transfer model. The excitation mechanism(s) for these levels is not described in the models. The observed transitions are labelled as ortho- or para-water in Fig. 1 and the calculated OPR values can be seen in Table 2. For each comet the OPR values determined agreed over the multiple offsets mentioned in Section 2 and therefore the values presented are an average over the observed nucleocentric distances. It should be noted that these offsets correspond to nucleocentric distances of ∼1000-10 000 km and the very inner comae of all comets are not observed.

As can be seen in Table 3, Hartley 2 has been studied previously and a wide range of OPR values have been determined (Crovisier et al. 1999; Dello Russo et al. 2011; Mumma et al. 2011; Bonev et al. 2013; Kawakita et al. 2013). The calculated value presented below agrees with the literature and gives a nuclear-spin temperature of ≈28 K.

By comparing the OPR values for Tempel 2 in Table 3, the OPR value reported in this study is a factor of 2 lower than previously seen (Paganini et al. 2012a) and results in a nuclear-spin temperature of ≈20 K. As both sets of observations were taken at similar r_h this suggests an OPR variation in the coma over the 16 d between observations. While this is an extreme case of OPR variation previous observations have seen an OPR variation from 2.5 to 1.8 in comet C/2001 A2 (LINEAR) (hereafter C/2001 A2) in 24 h (Dello Russo et al. 2005). Possible causes of OPR variation are presented in Section 1 and discussed in Section 4.1.
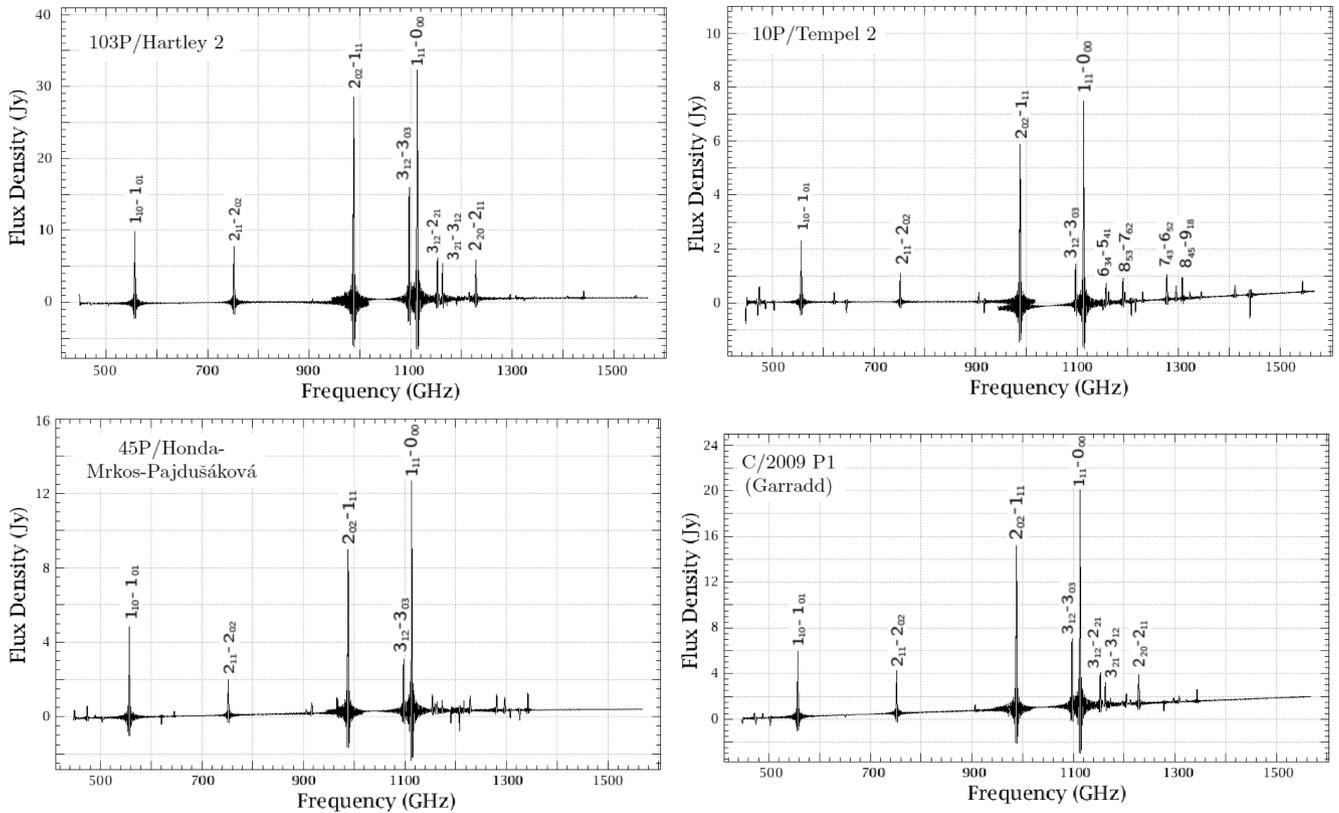
Figure 1. On-nucleus spectra obtained with SPIRE showing the fundamental rotational water lines and frequencies: $1_{10} - 1_{01}$ (557 GHz, Ortho), $2_{11} - 2_{02}$ (752 GHz, Para), $2_{02} - 1_{11}$ (988 GHz, Para), $3_{12} - 3_{03}$ (1097 GHz, Ortho), $1_{11} - 0_{00}$ (1113 GHz, Para), $3_{12} - 2_{21}$ (1153 GHz, Ortho), $6_{34} - 5_{41}$ (1158 GHz, Ortho), $3_{21} - 3_{12}$ (1163 GHz, Ortho), $8_{53} - 7_{62}$ (1191 GHz, Para), $2_{20} - 2_{11}$ (1229 GHz, Para), $7_{43} - 6_{52}$ (1278 GHz, Ortho), $8_{45} - 9_{18}$ (1308 GHz, Ortho).
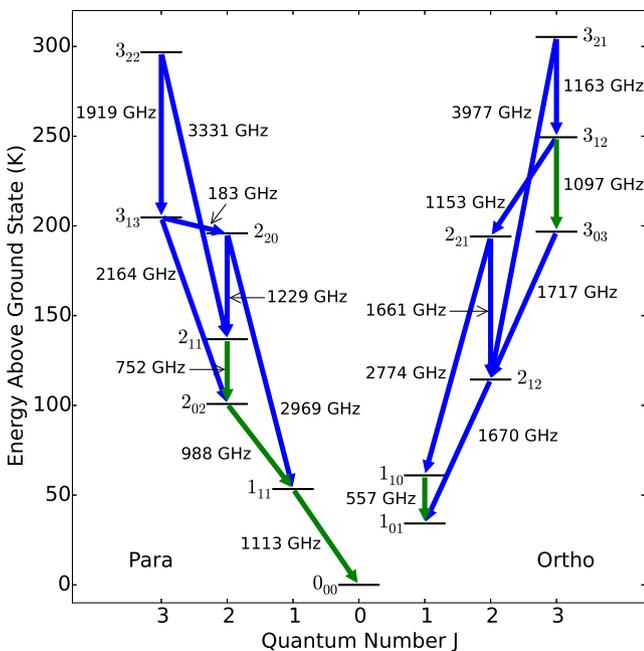
Figure 2. Ortho- and para-water transitions in the CRETE radiative transfer model, unobserved (blue arrows) and observed in all SPIRE detectors (green arrows).

For both 45P and C/2009 P1 no previous OPR determinations have been calculated. The determined OPR values for these comets reported in this study correspond to a nuclear-spin temperature of ≈22 K and ≈18 K, respectively. While the OPR values presented in Table 2 are lower than previously observed in comets, they agree with previous OPR values seen in 1P/Halley and C/2001 A2 (Mumma et al. 1988; Dello Russo et al. 2005).

3.3 Water production rates

The Q_{H_2O} values were calculated by comparing the radiative transfer model and observed line intensities via a least-squared fitting method over a Q_{H_2O} range of three decades. Q_{H_2O} values were determined using the calculated OPR values shown in Table 2. Typical values of the OPR in comets are 2.5–3.0 (de Val-Borro et al. 2010), and so Q_{H_2O} values were calculated for comets using an assumed OPR value of 3 in order to draw comparisons. These are presented in Table 2.

The Q_{H_2O} values for Hartley 2 vary in the range $2 - 8 \times 10^{27}$ s^{-1} for the calculated OPR and $2 - 9 \times 10^{27}$ s^{-1} for an OPR =3. Aside from the value determined from the $3_{12} - 3_{03}$ line, that is roughly an order of magnitude lower than for other transitions, these values are roughly equal to those calculated previously for observations taken at similar r_h as can be seen in Table 3 (Crovisier et al. 1999; Combi et al. 2011b; Dello Russo et al. 2011; Meech et al. 2011; Mumma et al. 2011; Kawakita et al. 2013; Knight & Schleicher 2013; Gicquel et al. 2014).

For Tempel 2 the Q_{H_2O} values presented here vary by an order of magnitude, $2 - 12 \times 10^{27}$ s^{-1} for the calculated OPR and

Table 3. OPR and Q_{H_2O} values determined from observations taken at similar r_h.

Comet	Apparition	r_{hobs} (au)	OPR	Q_{H_2O} (10^{27} s^{-1})	References
Hartley 2	2010	1.07	2.44 ± 0.71	1.89–7.46	1
			3	2.19–8.67	1
	1991	0.96	–	$\approx$63.00	2
		1.05	–	32.36	3
	1997	1.04	–	31.00 ± 2.00	4
		1.04	2.76 ± 0.08	12.40 ± 2.00	5
		1.06	–	15.14	3
		1.11	2.63 ± 0.18	5.40 ± 2.00	5
		1.17	–	18.80	6
	2010	1.06	3.4 ± 0.6	8.84–14.00	7
		1.06	2.76 ± 0.15	8.44–13.60	8
		1.06	–	11.48	3
		1.06	2.85 ± 0.20	6.78 ± 0.26	9
		1.07	–	7.56 ± 0.08	10
		1.07	–	7.32 ± 0.95	11
		1.07	2.88 ± 0.17	7.60–16.20	8
		1.07	–	$\approx$10.00	12
Tempel 2	2010	1.42	1.59 ± 0.23	2.2–11.6	1
			3	1.8–15.8	1
	1988	1.41	–	48.7	6
	1988	1.42	–	$\approx$15.0–20.0	13
	2010	1.42	–	$\approx$20.0	14
	2010	1.43	–	22.0 ± 1.0	15
	2010	1.44	3.01 ± 0.18	19.0 ± 1.2	16
45P	2011	1.00	2.00 ± 0.30	0.60–1.36	1
			3	0.90–2.04	1
	1995	1.14	–	1.92	6
	2011	1.03	–	0.91	17
C/2009 P1	2011	1.81	1.36 ± 0.22	69–255	1
			3	114–196	1
	2011	1.73	–	108 ± 30	18
		1.76	–	69–81	18
		1.80	–	270 ± 3	19
		1.84	–	90–106	20
		1.88	–	155–262	21
		2.00	–	46 ± 8	22
		2.00	–	84 ± 7	23
		2.10	–	86 ± 7	24

References. (1) This work; (2) Weaver et al. (1994); (3) Knight & Schleicher (2013); (4) Colangeli et al. (1999); (5) Crovisier et al. (1999); (6) Fink (2009); (7) Dello Russo et al. (2011); (8) Kawakita et al. (2013); (9) Mumma et al. (2011); (10) Combi et al. (2011b); (11) Gicquel et al. (2014); (12) Meech et al. (2011); (13) Roettger et al. (1990); (14) Szutowicz et al. (2011); (15) Biver et al. (2012); (16) Paganini et al. (2012a); (17) Lis et al. (2013b); (18) Bockelée-Morvan et al. (2014); (19) Combi et al. (2013); (20) DiSanti et al. (2014).; (21) Bockelée-Morvan et al. (2012); (22) Feaga et al. (2014); (23) Paganini et al. (2012b); (24) Villanueva et al. (2012).

$2 - 16 \times 10^{27}$ s^{-1} for OPR $=3$. By comparing these results with previous works Table 3 shows that the upper values from these observations are a factor of 2–4 lower than previously found (Roettger et al. 1990; Fink 2009; Szutowicz et al. 2011; Biver et al. 2012; Paganini et al. 2012a).

As can be seen in Table 3 the Q_{H_2O} values for 45P presented here, $0.6 - 1.4 \times 10^{27}$ s^{-1} and $0.9 - 2 \times 10^{27}$ s^{-1} for the calculated OPR and OPR $=3$, respectively, agree well with previous work observed at a similar time (Fink 2009; Lis et al. 2013b).

Values for Q_{H_2O} in the range $0.7 - 2.6 \times 10^{29}$ s^{-1} and $1.1 - 2.0 \times 10^{29}$ s^{-1} for the calculated OPR and OPR $=3$ respectively for C/2009 P1 were determined. These also agree well with the values presented in previous studies (Bockelée-Morvan et al. 2012; Paganini et al. 2012b; Villanueva et al. 2012; Combi

et al. 2013; Bockelée-Morvan et al. 2014; DiSanti et al. 2014; Feaga et al. 2014).

Q_{H_2O} values that are obtained from different transitions and offsets exhibit several features: (i) for Tempel 2, the rates calculated from all transitions are approximately similar, (ii) for Hartley 2, the rate determined from the $3_{12} - 3_{03}$ line is significantly lower than observed from other transitions, (iii) for 45P and C/2009 P1, the rates calculated from the $3_{12} - 3_{03}$ and $2_{11} - 2_{02}$ lines are both noticeably lower than that determined from other transitions, and (iv) for all comets there is evidence of a trend for Q_{H_2O} to *decrease* with increasing offset.

For comets with an observed OPR lower than the canonical, statistical equilibrium value of 3, the Q_{H_2O} values are higher for ortho-water lines and lower for para-water lines. For Hartley 2,

whose calculated OPR is slightly higher than 3, the reverse is true. This is as expected, because in order to reproduce the observed line intensities a higher ortho-Q_{H_2O} (and lower para-Q_{H_2O}) would be needed if the OPR is lower than the statistical equilibrium value.

Significantly, for the majority of the observed comets, the use of these OPR values also results in a more consistent, narrower range of Q_{H_2O} values as determined from different transitions in each comet. This gives some support for the adoption of these OPR values. As can be seen in Table 2, even for low OPR values, the Q_{H_2O} values do not differ from those determined using an OPR =3 by more than a factor of 2.

4 DISCUSSION

4.1 OPR variation

One of the main results of this study is that the observed OPRs of three of the comets, Tempel 2, 45P and C/2009 P1, presented in Table 2, are considerably lower than the statistical equilibrium value of 3. However, as has been mentioned above, these values do agree with the OPR observed in other comets and interestingly they agree well with values found in the protoplanetary disc TW Hydrae that has a range of OPR from 0.73 to 1.52 depending on the disc model (Salinas et al. 2016). Previously, an OPR of less than 3 was thought to be due to a lower comet ice formation temperature; however recent laboratory studies have shown that solid-phase rapid nuclear-spin conversion equilibrates the OPR and gas-phase nuclear-spin conversion processes mentioned previously may be the cause of the OPR variation seen (Hama et al. 2016).

Previous observations of Tempel 2 were taken at lower nucleocentric distances than the observations presented here (Paganini et al. 2012a). The observations were centred on the nucleus, extending up to 1500 km. As previously mentioned, laboratory results seem to suggest that the Tempel 2 OPR previously determined is due to rapid nuclear-spin conversion normalizing the OPR to the statistical equilibrium and the observed post-sublimation OPR value was 3. Whereas the OPR presented here was observed at a greater nucleocentric distance suggesting that nuclear-spin conversion via proton-transfer reactions of water with H^+ and H_3O^+ or water molecule collisions with water clusters, ice grains or paramagnetic dust grains has occurred.

It should also be noted that the Hartley 2 OPR values taken from the literature were determined from observations centred on-nucleus and extending up to several hundred km. All OPR values roughly agree with the statistical equilibrium OPR value of 3. For the SPIRE observations presented here, the on-nucleus OPR values for all comets in this study agree with the coma OPR value reported in Table 2. Assuming rapid nuclear-spin conversion occurs in the solid-phase on the nucleus, then due to the relatively large SPIRE beam sizes coma nuclear-spin conversion is being observed at nucleocentric distances less than $\sim 1000 - 10000$ km.

One of the first determinations of a cometary OPR was in comet C/1995 O1 (Hale–Bopp) in 1996 using ISO (Crovisier et al. 1997). An OPR of 2.45 ± 0.10 was reported using on-nucleus observations that extended up to roughly 20 000 km suggesting that if the OPR of sublimated water should be equal to 3 then the ISO observation has also observed water that has undergone nuclear-spin conversion in the coma.

Interestingly, observations of the very inner coma of 73P-B/Schwassmann-Wachmann 3 and inner coma of C/2004 Q2 (Machholz) determined an OPR of roughly 3 and showed no variation over nucleocentric distances of 5–30 km and $\leq$1000 km,

respectively (Bonev et al. 2007, 2008). Furthermore, on-nucleus observations extending up to a nucleocentric distance of 350–1700 km taken of C/1999 H1 (Lee), C/1999 S4 (LINEAR) and C/2001 A2 (LINEAR) roughly agree with a statistical equilibrium OPR value. However, an OPR variation from 2.5 to 1.8 was seen in C/2001 A2 (LINEAR) from observations at the same nucleocentric and similar heliocentric distances suggesting nuclear-spin conversion via the processes mentioned above was observed (Dello Russo et al. 2005).

It should also be noted that no significant difference in OPR for comets from the different comet families was seen. This is consistent with a recent study of ammonia in 26 comets (Shinnaka et al. 2016).

These observations seem to further support rapid solid-phase nuclear-spin conversion in cometary ice. However, these results highlight the need for further study of nuclear-spin conversion in cometary comae as it has previously been proposed that the processes mentioned above would occur in the very inner coma, but from the analysis above it would seem that OPR variation could occur at a range of nucleocentric distances.

4.2 Water production rate variation

The variation of Q_{H_2O} with offset position is difficult to explain and there are a number of possible causes.

(i) The temperature is not constant, but varies with position as line intensities are sensitive to the gas temperature profile in the inner coma.

(ii) There is an extra source of water in comae, perhaps from the sublimation of the dust ice mantles.

(iii) There is a spatial variation in the OPR.

(iv) The assumption of spherical symmetry in the radiative transfer model, both with respect to the outflow profile and the treatment of the photolysis reactions, may not be correct.

(v) The excitation model for the water transitions may be over-simplified and/or missing key processes such as transitions from higher rotational levels.

There is insufficient spatial resolution/data points to discriminate between these possibilities, but the strong discrepancy between the Q_{H_2O} values inferred from the $3_{12} - 3_{03}$ (and $2_{11} - 2_{02}$) lines and the other transitions suggests that an over-simplified model may be at least part of the cause of the observed variations. Furthermore, the pattern of the Q_{H_2O} variations varies from source to source and transition to transition, suggesting that temperature variation may not be the sole cause of the variation.

Note that the only Oort-cloud comet (C/2009 P1) in this study has a range of Q_{H_2O} values of at least an order of magnitude higher than the Jupiter-family comets. By comparing the determined Q_{H_2O} values in this study with other comets, C/2009 P1 has the second highest Q_{H_2O} at the observed r_h. Comet C/1995 O1 (Hale–Bopp) was observed to have a Q_{H_2O} an order of magnitude higher (Combi et al. 2000). Interestingly, 45P has the lowest known Q_{H_2O} at the observed r_h. Comet 67P/Churyumov–Gerasimenko has a similarly low Q_{H_2O} at a slightly greater r_h (Bertaux et al. 2014), although the observed values vary considerably with little change in r_h.

From the comparisons above and the fact that two comets in this study (Hartley 2 and Tempel 2) have lower Q_{H_2O} values than any Oort-cloud comet at the observed r_h, one could draw the conclusion that Oort-cloud comets have greater Q_{H_2O} values due to a combination of a greater retention of accreted volatiles during formation and fewer perihelion passes. While in general this seems to be true, there are exceptions as 1P/Halley and 21P/Giacobini–Zinner have higher Q_{H_2O} values than C/2011 L4 (PanSTARRS) and C/2012 S1

(ISON) at similar observed r_h (Combi & Feldman 1993; Combi et al. 2011a, 2014a,b). Although this could be due to the nuclei of 1P/Halley and 21P/Giacobini–Zinner being larger than C/2012 S1 (ISON) and C/2011 L4 (PanSTARRS) (Ferrín 2014).

Furthermore, 19P/Borrelly has a Q_{H_2O} approximately a factor of 2 greater than C/1997 T1 (Utsunomiya) at a similar observed r_h (Mäkinen et al. 2001; Combi et al. 2011a). Although no definite r_n for C/1997 T1 (Utsunomiya) has been calculated, an upper limit of 5.8 km has been determined (Fernandez 1999), whereas 19P/Borrelly has a r_n of 1.9 km (Lowry, Fitzsimmons & Collander-Brown 2003). If the r_n of C/1997 T1 (Utsunomiya) is equal, or greater, to that of 19P/Borrelly then comet family might not influence Q_{H_2O}; however if the nucleus radius of the Oort-cloud comet is much lower than 1.9 km then there would be more evidence that comet family affects Q_{H_2O}.

By looking at Table 3 another interesting point can be noted. The Q_{H_2O} values of Hartley 2, Tempel 2 and 45P for previous apparitions are higher at similar observed r_h than values presented in this study. Indeed, for Hartley 2 a difference in Q_{H_2O} after one orbit can be seen between the 1991 and 1997 apparitions at $r_h = 1.04 - 1.06$ au. For 45P the Q_{H_2O} value during the 1995 apparition is $\approx 1.5 - 3$ times greater than the value reported in this study for a greater r_h, therefore strengthening the idea that in general Oort-cloud comets have a greater Q_{H_2O} due to fewer perihelion passes.

5 CONCLUSIONS

Using spectroscopic observations taken by *Herschel*/SPIRE OPR values of three Jupiter-family comets and one Oort-cloud comet were determined. While the OPR for Hartley 2 is consistent with previous studies, the value calculated for Tempel 2 is lower than previously observed. The observed variation from the literature value could be due to gas-phase nuclear-spin conversion in the coma that occurred post-OPR equilibrium in the solid-phase on the nucleus and sublimation. The first OPR values for 45P and C/2009 P1 are presented. Although the OPR values for all comets aside from Hartley 2 are amongst the lowest observed, they agree with OPRs determined from previous observations of comets 1P/Halley and C/2001 A2, and the protoplanetary disc TW Hydrae. An important result of this study is that the observations are consistent with the findings of recent laboratory studies and that the OPR values presented provide good evidence of post-sublimation gas-phase nuclear-spin conversion.

From the OPR values the nuclear-spin temperatures of the four comets were determined and there was no substantial difference in the nuclear-spin temperatures for comets from different families.

An established radiative transfer model and the calculated OPR values were used to determine Q_{H_2O} values, that vary with OPR as expected.

Q_{H_2O} values generally agree within an order of magnitude with previous observations; however notable exceptions are that the Q_{H_2O} values for all four comets determined from the $3_{12} - 3_{03}$ ortho-water line (and for two comets, the $2_{11} - 2_{02}$ para-water line) are lower. Consistently lower values across all four comets could suggest potential level population inaccuracies in the model; however further work is needed into this.

In general, the Q_{H_2O} values decrease with increasing offset from the comet. There are a number of possible explanations for this, but inaccuracies in the excitation model are potentially the most likely cause.

In this survey the only Oort-cloud comet, C/2009 P1, has a Q_{H_2O} value one-two orders of magnitude higher than the Jupiter-family comets. Placing the results reported here in context with the literature, C/2009 P1 has one of the highest Q_{H_2O} values at the observed r_h and that the three Jupiter-family comets have some of the lowest Q_{H_2O} values seen. One could conclude that Q_{H_2O} is related to comet family and therefore formation conditions. However, as mentioned previously there are potential exceptions that put this relationship into doubt. The Q_{H_2O} values for the three Jupiter-family comets in this study have been seen to decrease from previous apparitions suggesting Oort-cloud comets have a greater Q_{H_2O} due to fewer perihelion passes.

REFERENCES

Altwegg K. et al., 2015, Science, 347, 1261952
Balsiger H., 1990, in Mason J. W., ed., Measurements of Ion Species within the Coma of Comet Halley from Giotto. Ellis Horwood Ltd., p. 129
Bensch F., Bergin E. A., 2004, ApJ, 615, 531
Bertaux J.-L., Combi M. R., Quémerais E., Schmidt W., 2014, Planet. Space Sci., 91, 14
Biver N., 1997, PhD thesis, Univ. Paris 7-Diderot
Biver N. et al., 2007, Planet. Space Sci., 55, 1058
Biver N. et al., 2009, A&A, 501, 359
Biver N. et al., 2012, A&A, 539, A68
Bockelée-Morvan D. et al., 2012, A&A, 544, L15
Bockelée-Morvan D. et al., 2014, A&A, 562, A5
Bockelée-Morvan D. et al., 2015, Space Sci. Rev., 197, 47
Bonev B. P., Mumma M. J., Villanueva G. L., Disanti M. A., Ellis R. S., Magee-Sauer K., Dello Russo N., 2007, ApJ, 661, L97
Bonev B. P., Mumma M. J., Kawakita H., Kobayashi H., Villanueva G. L., 2008, Icarus, 196, 241
Bonev B. P., Villanueva G. L., Paganini L., DiSanti M. A., Gibb E. L., Keane J. V., Meech K. J., Mumma M. J., 2013, Icarus, 222, 740
Buntkowsky G. et al., 2008, Z. Phys. Chem., 222, 1049
Choi Y., van der Tak F. F. S., Bergin E. A., Plume R., 2014, A&A, 572, L10
Colangeli L. et al., 1999, A&A, 343, L87
Combi M. R., Feldman P. D., 1993, Icarus, 105, 557
Combi M. R., Cochran A. L., Cochran W. D., Lambert D. L., Johns-Krull C. M., 1999, ApJ, 512, 961
Combi M. R., Reinard A. A., Bertaux J.-L., Quemerais E., Mäkinen T., 2000, Icarus, 144, 191
Combi M. R., Lee Y., Patel T. S., Mäkinen J. T. T., Bertaux J.-L., Quémerais E., 2011a, AJ, 141, 128
Combi M. R., Bertaux J.-L., Quémerais E., Ferron S., Mäkinen J. T. T., 2011b, ApJ, 734, L6
Combi M. R., Mäkinen J. T. T., Bertaux J.-L., Quémerais E., Ferron S., Fougere N., 2013, Icarus, 225, 740
Combi M. R., Bertaux J.-L., Quémerais E., Ferron S., Mäkinen J. T. T., Aptekar G., 2014a, AJ, 147, 126
Combi M. R., Fougere N., Mäkinen J. T. T., Bertaux J.-L., Quémerais E., Ferron S., 2014b, ApJ, 788, L7

Crovisier J., 1984, A&A, 130, 361

Crovisier J., Leech K., Bockelee-Morvan D., Brooke T. Y., Hanner M. S., Altieri B., Keller H. U., Lellouch E., 1997, Science, 275, 1904

Crovisier J. et al., 1999, in Cox P., Kessler M., eds, ESA Special Publication Vol. 427, The Universe as Seen by ISO. ESA-SP, p. 161

de Val-Borro M. et al., 2010, A&A, 521, L50

de Val-Borro M. et al., 2012, A&A, 546, L4

de Val-Borro M. et al., 2014, A&A, 564, A124

de Val-Borro M., Wilson T. G., 2016, CRETE: Comet RadiativE Transfer and Excitation. Astrophysics Source Code Library

Dello Russo N., Bonev B. P., DiSanti M. A., Mumma M. J., Gibb E. L., Magee-Sauer K., Barber R. J., Tennyson J., 2005, ApJ, 621, 537

Dello Russo N. et al., 2011, ApJ, 734, L8

DiSanti M. A., Villanueva G. L., Paganini L., Bonev B. P., Keane J. V., Meech K. J., Mumma M. J., 2014, Icarus, 228, 167

Feaga L. M. et al., 2014, AJ, 147, 24

Fernandez Y. R., 1999, PhD thesis, University of Maryland College Park

Ferrín I., 2014, MNRAS, 442, 1731

Festou M. C., 1990, Mason J. W., ed., Variations of the Gaseous Output of the Nucleus of Comet Halley. Ellis Horwood Ltd., p. 245

Fink U., 2009, Icarus, 201, 311

Gicquel A. et al., 2014, ApJ, 794, 1

Griffin M. J. et al., 2010, A&A, 518, L3

Gulkis S., 2014, Central Bureau Electronic Telegrams, 3912

Hama T., Watanabe N., 2013, Chem. Rev., 113, 8783

Hama T., Kouchi A., Watanabe N., 2016, Science, 351, 65

Hartogh P. et al., 2009, Planet. Space Sci., 57, 1596

Hartogh P. et al., 2010, A&A, 518, L150

Haser L., 1957, Bulletin de la Societe Royale des Sciences de Liege, 43, 740

Herschel Science Centre, 2014, SPIRE Handbook 2016, Herschel Explanatory Supplement vol. 2.5. HERSCHEL-DOC-0798

Hogerheijde M. R., van der Tak F. F. S., 2000, A&A, 362, 697

Irvine W. M., Schloerb F. P., Crovisier J., Fegley B., Jr, Mumma M. J., 2000, Protostars and Planets IV. University of Arizona Press, Tucson, p. 1159

Kawakita H. et al., 2013, Icarus, 222, 723

Knight M. M., Schleicher D. G., 2013, Icarus, 222, 691

Lecacheux A. et al., 2003, A&A, 402, L55

Lis D. C., Bergin E. A., Schilke P., van Dishoeck E. F., 2013a, J. Phys. Chem. A, 117, 9661

Lis D. C. et al., 2013b, ApJ, 774, L3

Lowry S. C., Fitzsimmons A., Collander-Brown S., 2003, A&A, 397, 329

Mäkinen J. T. T., Bertaux J.-L., Pulkkinen T. I., Schmidt W., Kyrölä E., Summanen T., Quémerais E., Lallement R., 2001, A&A, 368, 292

Manca Tanner C., Quack M., Schmidiger D., 2013, J. Phys. Chem. A, 117, 10105

Meech K. J. et al., 2011, ApJ, 734, L1

Mumma M. J., Weaver H. A., Larson H. P., 1987, A&A, 187, 419

Mumma M. J., Blass W. E., Weaver H. A., Larson H. P., 1988, BAAS, 20, 826

Mumma M. J. et al., 2011, ApJ, 734, L7

Neufeld D. A. et al., 2000, ApJ, 539, L107

Paganini L., Mumma M. J., Bonev B. P., Villanueva G. L., DiSanti M. A., Keane J. V., Meech K. J., 2012a, Icarus, 218, 644

Paganini L., Mumma M. J., Villanueva G. L., DiSanti M. A., Bonev B. P., Lippi M., Boehnhardt H., 2012b, ApJ, 748, L13

Pilbratt G. L. et al., 2010, A&A, 518, L1

Roettger E. E., Feldman P. D., A'Hearn M. F., Festou M. C., 1990, Icarus, 86, 100

Salinas V. N. et al., 2016, A&A, 591, A122

Shinnaka Y., Kawakita H., Jehin E., Decock A., Hutsemékers D., Manfroid J., 2016, MNRAS, 462, S124

Swinyard B. M. et al., 2014, MNRAS, 440, 3658

Szutowicz S. et al., 2011, in EPSC-DPS Joint Meeting 2011. held 2–7 October 2011 in Nantes, France, p. 1213

Villanueva G. L., Mumma M. J., DiSanti M. A., Bonev B. P., Paganini L., Blake G. A., 2012, Icarus, 220, 291

Weaver H. A., Feldman P. D., McPhate J. B., A'Hearn M. F., Arpigny C., Smith T. E., 1994, ApJ, 422, 374

Willacy K. et al., 2015, Space Sci. Rev., 197, 151

Zakharov V., Bockelée-Morvan D., Biver N., Crovisier J., Lecacheux A., 2007, A&A, 473, 303

This paper has been typeset from a TEX/LATEX file prepared by the author.